

DFT investigation of the influence of ordered vacancies on elastic and magnetic properties of graphene and graphene-like SiC and BN structures

A. S. Fedorov^{*1}, Z. I. Popov¹, D. A. Fedorov¹, N. S. Eliseeva², M. V. Serjantova², and A. A. Kuzubov²

¹Kirensky Institute of Physics, Siberian Branch of RAS, Krasnoyarsk 660036, Russia

²Siberian Federal University, Krasnoyarsk 660028, Russia

Received 30 April 2012, revised 15 August 2012, accepted 14 September 2012

Published online 29 October 2012

Keywords boron nitride, carbon silicide, elastic properties, graphene, magnetic properties, vacancies

* Corresponding author: e-mail alex99@iph.krasn.ru, Phone: +7-904-8985175, Fax: +7-391-243-89-23

Influence of ordered monovacancies on elastic properties of graphene is theoretically investigated by density functional theory (DFT) calculations. Inverse linear dependence of the graphene Young's modulus on the concentration of vacancies has been revealed and migration rate of the vacancies has been calculated as a function of applied strain. It is shown that the migration rate can be controlled by applying various strains or temperatures. The influence of ordered monovacancies on magnetic properties

of graphene as well as graphene-like hexagonal carbon silicide (2D-SiC) and the boron nitride (h-BN) structures is investigated. It is established that the presence of vacancies in all systems yields the appearance of local magnetic moment. However, in 2D-SiC structure the magnetic moment occurs only in the case of a Si vacancy. Influence of the distance between vacancies on the ferromagnetic or anti-ferromagnetic ordering for all structures is established.

© 2012 WILEY-VCH Verlag GmbH & Co. KGaA, Weinheim

1 Introduction Since 2004, graphene has been proved to be an exciting new material [1] because of its unique optical, electrical, and mechanical properties [2]. Graphene has a high mobility of electrons and holes and it is one of the most elastic and strong materials with a Young's modulus of about 1 TPa [3]. Lattice defects obviously affect on the electronic and elastic properties, so defects and their influence on the properties were studied intensively. Vacancies, which usually appear in the process of ion or electron bombardment of graphite or carbon nanotubes, have been studied by many researchers [3, 4]. Various experimental methods were used to study the structure and properties of vacancies in graphite and carbon nanotubes. It was found that vacancies generated in electron-irradiated carbon nanotubes can lead to structural changes [5, 6]. Structure and diffusion of vacancies were investigated in a number of theoretical works [4, 7–9], whereas dynamics of vacancies and their effect on the elastic properties of graphene, especially for the strained state, have not been considered yet. The next important question of graphene's physics is the possibility of magnetism existence in the

systems without d- or f-electrons. Magnetic moments generated in proton-irradiated graphite were detected in experimental works [10, 11]. This effect was explained by crystalline [12–15] and structural defects [16]. Authors of Ref. [17] show that there are local magnetic moments around the vacancies and it is possible to make graphene-based magnetic material, where even ferro-antiferro transition is possible [18]. The nature of the vacancies' magnetic moments in graphite and graphene was theoretically studied in Refs. [19–20]. As well as graphene, similar hexagonal planar structures 2D-SiC and h-BN can have magnetic moments, occurring due to presence of vacancies. DFT-GGA spin-polarized calculations of 2D-SiC [21] showed that Si and C vacancies play different role in the magnetism formation. Although Si vacancy (V_{Si}) leads to local magnetic moment, but C vacancy (V_C) does not. The absence of the magnetic moment can be explained by the lattice local deformation. As Si atomic radius is larger than C radius, it is possible a weak bond between Si atoms surrounding the vacancy is formed. It leads to the formation of associated electron pairs and an absence of the magnetic moments. This

effect is typical also for cubic (3C-SiC) crystal [22]. Mentioned in the previous paper, the authors indicate the presence of two configurations of V_{Si} having magnetic moments of 4.0 and 1.9 μ_B , corresponded to high and low spin states, respectively. The calculation results show that the low-spin state is energetically more favorable by 0.039 eV and the spin-density distribution in the low-spin state is as follows: two of the three atoms have the same spin directions, but the third atom has opposite one. A monolayer of h-BN with vacancies is one more example of the magnetization occurrence in the planar structures [23, 24]. In Ref. [23] six types of defects in the h-BN monolayer were theoretically studied within DFT-GGA approach: B and N vacancies, the substitution of B atoms by N atoms and vice versa, and the substitution of boron or nitrogen atom by carbon. At that spontaneous magnetization in the presence of vacancies and substitutional impurities was detected. In the presence of B or N vacancies the magnetic moments of 3.0 and 1.0 μ_B , respectively, were found. This difference can be explained by the fact that when the nitrogen atom is removed from the h-BN cell there is only one unpaired electron but when the B atom is removed there are three such electrons. From the facts above it can be concluded that a single vacancy's appearance in the graphene, 2D-SiC and h-BN monolayers can lead to the magnetic moments occurrence. However, the question about the presence of magnetic order in the case of high vacancies' concentration remains unclear. One of this work goals was to investigate the effect of the different concentration of ordered monovacancies on the graphene elastic properties and on the vacancies' migration rate under a strain or temperature influence. Another goal was to investigate the magnetic moments and their localization of ordered vacancies in the graphene, 2D-SiC and h-BN monolayers. Also an influence of the distance between vacancies on the ferromagnetic-antiferromagnetic ordering was studied.

2 Investigation method The calculations were performed within the framework of the density functional theory (DFT) with the gradient corrections PBE using the Vienna *ab initio* simulation package (VASP) [25, 26]. This package is based on the pseudopotential method and the expansion of wavefunctions in the plane wave basis. To efficiently reduce the number of basis functions and to increase the calculation rate, the Vanderbilt ultrasoft pseudopotentials were used for all atoms [27]. For the first Brillouin zone (1BZ) integration, the special k -points of the Monkhorst–Pack scheme [28] were chosen. Because of quite large supercells' sizes of all structures, the only 4 k -points inside irreducible part of 1BZ were used for all cases. For the graphene a geometry was optimized until pressure and forces acting on each atom become less than 1 kbar and 0.05 eV \AA^{-1} correspondently. We have determined that these values were sufficient for a correct description of the lattice parameters ($a_{\text{exp}} = 2.461 \text{ \AA}$ vs. $a_{\text{calc}} = 2.46 \text{ \AA}$). Also these values were sufficient for calculation of the elastic properties of the graphene with or without vacancies, see below. For all other

systems the pressure and forces acting on atoms during optimization not exceed 1 kbar and 0.01 eV \AA^{-1} ensure good convergence with respect to the cell parameters and magnetic properties. For example, calculated cell parameter a of h-BN was equal 2.504 \AA while experimental value $a = 2.500\text{--}2.504 \text{ \AA}$, see Ref. [29].

3 Graphene's elastic properties investigation To determine the vacancies influence on the elastic properties of the graphene, we successively chose a number of rectangular and almost square supercells consisting of 60, 128, 180, and 336 carbon atoms, where one atom is replaced by the monovacancy. The supercell dimension along the z -axis was 15 \AA in all cases, which ensured the absence of chemical interactions with periodically located plane images. The rectangular unit cell shape allows to calculate linear elastic Young's moduli Y_{xx} and Y_{yy} by the corresponding strains in the x and y directions. The choice of the square cell ensured the equidistance of vacancies from each other and reduce the cell shape influence on the elastic moduli calculations. To determine the elastic moduli σ_{xx} and σ_{yy} we successively apply small strains within $\pm 3\text{--}6\%$ along x and y directions. Under fixed deformation along one axis, the cell size along another axis was varied to ensure zero total pressure along this axis. The calculated Young's moduli of defect-free graphene for deformations in the x and y directions are 1.02 and 0.98 TPa, respectively, which are in agreement with an experimental value of 1.0 TPa [3]. Calculated ratios of the Young's moduli Y_{xx} and Y_{yy} for structures with a vacancy to the respective moduli for the defect-free structure are shown in Fig. 1 as functions of the distance between vacancies. One can see the both Young's moduli of graphene with periodically located vacancies are monotonically increasing with the increasing of distance between vacancies. When the distance between the vacancies of about 30 \AA , the both Young's moduli are almost equal to the moduli of the defect-free graphene. In the figure one can see the intersections of the Y_{xx} and Y_{yy} curves, what can be explained by different interaction of the vacancies located in neighboring supercells under armchair and zigzag

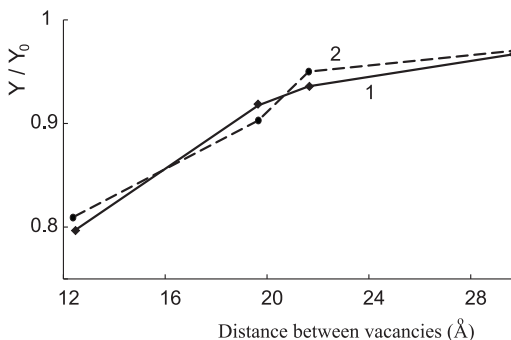


Figure 1 Ratio of the Young's modulus Y_{xx} (1) and Y_{yy} (2) for graphene with vacancies to the Young's modulus Y_0 for defect-free graphene in the cases of deformations along the x and y axes versus the distance between periodic vacancies.

directions. We also calculated the dependences of the graphene vacancy's hopping rate ν through the potential barriers E_b on the applied strains and temperature T . For that we used transition state theory and Arrhenius-like formula $\nu = \nu_0 \exp(-\frac{E_b}{kT})$. The potential barriers E_b for an atom jump into nearest vacancy under different strains were calculated by the nudged elastic band method (NEB) [30]. The preexponential factor ν_0 was calculated by the well-known Vineyard formula [31]:

$$\nu_0 = \frac{kT}{\hbar} \frac{\prod_{i=1}^{3N-3} \nu_i}{\prod_{i=1}^{3N-4} \nu'_i},$$

where ν_i and ν'_i are the vibration frequencies of N atoms when the transferred atom is in the potential minimum and in the saddle point of the potential relief, correspondently. The all frequencies were calculated by the frozen phonon method. Due to large size of the system, only the degrees of freedom of the transferred atom and its four nearest neighbors were taken into account. This simplification of the Vineyard formula for calculating of the hopping rate was tested in Ref. [32]. It was found that the potential barrier's heights for the motion of the vacancies strongly depend on the applied strain. For example, the potential barrier is 1.17 eV for the strain absence and is 1.79 and 0.12 eV for the 5% compression strain along x and y axes, respectively. This means that vacancy's hopping rate both increases and decreases, except for the shear strain, by several orders of magnitude under small strains. This strong dependence can be used for the directional movement of the graphene vacancies in a nonuniform strain field.

4 Magnetic properties investigation For that the hexagonal unit cells consisting of two atoms were constructed for the graphene, 2D-SiC and h-BN. Then the supercells consisting of $6 \times 6 \times 1$, $8 \times 8 \times 1$, and $10 \times 10 \times 1$ unit cells were considered. Every supercell was consisted of four equivalent miniblocks containing a vacancy and having $3 \times 3 \times 1$, $4 \times 4 \times 1$, and $5 \times 5 \times 1$ unit cells. Such geometry allows to research antiferromagnetic configuration where magnetic moments of vacancies in neighboring miniblocks have different sign.

We investigated the ferromagnetic, antiferromagnetic, and nonmagnetic states of the graphene, 2D-SiC, and h-BN supercells with four vacancies. To do that the spin-polarized and non-spin-polarized calculations were carried out. Ferromagnetic state was obtained by setting the same initial magnetic moments on all atoms and further electronic iterations. For the 2D-SiC structure a low-spin state has been obtained, which is energetically more favorable than high-spin state, in agreement with [21]. Antiferromagnetic states for all supercells were specified by the initial alternation of the magnetic moment signs of the vacancies in the nearest miniblocks and further electronic iterations.

The results for magnetic properties of the graphene, 2D-SiC, and h-BN supercells with four vacancies are shown in Table 1. It can be seen that magnetic configurations have a

Table 1 Magnetic ordering of the graphene, 2D-SiC, and h-BN structures. R – distance between vacancies (\AA); S_{eff} – effective magnetic moment of the vacancy; $\Delta E_{\text{F-AF}}$ – energy difference between ferro- and antiferro configurations, per supercell; $\Delta E_{\text{nm-m}}$ – total energy difference between nonspinpolarized and spinpolarized calculations, per supercell.

| structure | R | S_{eff} | $\Delta E_{\text{F-AF}}$ | $\Delta E_{\text{nm-m}}$ |
|--------------------------|------|------------------|--------------------------|--------------------------|
| graphene with vacancies | 7.4 | 1.4 | 0.0064 | 1.564 |
| | 9.8 | 1.1 | 0.0047 | 1.798 |
| | 12.2 | 1.1 | -0.0146 | 1.556 |
| 2D-SiC with Si vacancies | 9.2 | 1.6 | 0.0543 | 0.680 |
| | 12.3 | 1.6 | -0.0592 | 1.330 |
| | 15.4 | 1.5 | 0.0022 | 1.535 |
| h-BN with B vacancies | 7.5 | 1.7 | 0.3378 | 0.139 |
| | 10.0 | 2.2 | -0.0670 | 0.984 |
| | 12.5 | 2.3 | -0.0323 | 1.183 |
| h-BN with N vacancies | 7.5 | 0.9 | -0.0079 | 0.217 |
| | 10.0 | 0.9 | 0.0080 | 0.257 |
| | 12.5 | 0.9 | 0.0007 | 0.288 |

significantly lower total energy than nonmagnetic configurations that means the vacancies have a nonzero magnetic moments for all systems, except 2D-SiC structure with C vacancies. Also it is obvious that ferro- or antiferro configurations may differ in stability at different distances between vacancies. It can be explained by the fact that the sign of the exchange integrals between the vacancies effective magnetic moments are changed when the distance between vacancies is changed. This exchange integral dependence on distance can be explained by the Ruderman–Kittel–Kasuya–Yosida (RKKY) mechanism. Convincing evidence of the exchange integrals sign change was shown in Ref. [33], where model Green function calculations were performed for periodical local magnetic impurities in the graphene, located at different distances between them.

Our calculations showed that the graphene with vacancies has the following peculiarity: two of three atoms surrounding the vacancy get closer to each other with weak-coupling formation. It was established that the atoms

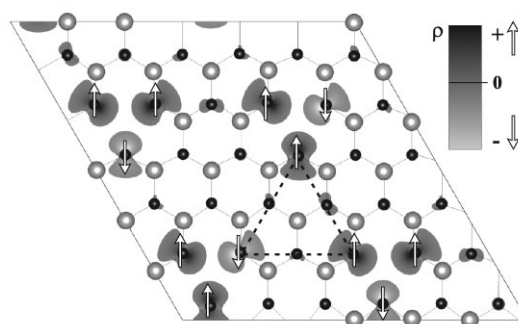


Figure 2 Spin density $\rho(r)$ for ferromagnetic state of 2D-SiC; black balls – C atoms, gray balls – Si atoms; dashed lines indicate the second coordination sphere of the vacancy.

